Dynamic stress response of track layers under high speed trains

Réponse dynamique au stress dans les couches de voie sous les trains à grande vitesse

Rakesh Sai Malisetty, Buddhima Indraratna, Ameyu Tucho & Trung Ngo
School of Civil and Environmental Engineering, University of Technology Sydney, Australia,
rakeshsai.malisetty@uts.edu.au

ABSTRACT: Dynamic stress response under high-speed trains in track substructure layers such as ballast, capping, and subgrade are often associated with the generation and propagation of Rayleigh waves in the track. It is vital to estimate the critical train speed (V_c) for a track, at which the dynamic response becomes maximum. Moreover, an understanding of the dynamic stress state and stress paths in ballast layer induced by high-speed trains is essential to the track design. In this paper, a simple analytical model is presented to investigate the dynamic stress response in ballast layer at different train speeds for passenger and heavy haul axle loads. The analytical model is used to analyse the critical speed (V_c) of the track system by considering the wave propagation in ballast as well as subgrade layers. The influence of different parameters such as stiffness of track layers, ballast fouling and thickness of the ballast layer on the dynamic stresses in ballast layer are analysed. Though V_c does not change with increasing the axle load, the dynamic stresses in the ballast layer are found to be higher for freight trains compared to passenger trains. When these dynamic stresses are compared with the peak static strength of ballast, the limiting train speed (V_l) for optimal performance of ballast layer is found to be much lower than V_c.

RÉSUMÉ: La réponse dynamique aux contraintes sous les trains à grande vitesse dans les couches de sous-structure de la voie, telles que le ballast, le recouvrement et la plate-forme, est souvent associée à la génération et à la propagation des ondes de Rayleigh dans la voie. Il est essentiel d'estimer la vitesse critique du train (V_c) pour une voie, à laquelle la réponse dynamique devient maximale. De plus, une compréhension de l'état de contrainte dynamique et des chemins de contrainte dans la couche de ballast induits par les trains à grande vitesse est essentielle à la conception de la voie. Dans cet article, un modèle analytique simple est présenté pour étudier la réponse dynamique aux contraintes dans la couche de ballast à différentes vitesses de train pour les charges des essieux passagers et lourds. Le modèle analytique est utilisé pour analyser la vitesse critique (V_c) du système de voie en considérant la propagation des ondes dans le ballast ainsi que dans les couches de fondation. L'influence de différents paramètres tels que la rigidité des couches de voie, l'encrassement du ballast et l'épaisseur de la couche de ballast sur les contraintes dynamiques dans la couche de ballast est analysée. Bien que V_c ne change pas avec l'augmentation de la charge à l'essieu, les contraintes dynamiques dans la couche de ballast sont plus élevées pour les trains de marchandises que pour les trains de passagers. Lorsque ces contraintes dynamiques sont comparées à la résistance statique maximale du ballast, la vitesse limite du train (V_l) pour des performances optimales de la couche de ballast se révèle être bien inférieure à V_c.

KEYWORDS: ballasted railway track, stress amplification, critical speed

1 INTRODUCTION

High-speed trains have become an efficient way of passenger transportation in the 21st century. High-speed rail corridors are already operational in several countries across the world. Even though these corridors are dominated by ballast-less slab tracks (e.g., China), many countries like Japan and France use ballasted tracks. The relatively low initial construction costs and the convenience of already existing ballasted railway tracks for running high-speed and freight transport are the main advantages of ballasted railway tracks. For these types of tracks, significant improvement of the track layers and embankment is required before increasing the operational speeds. The major challenge while increasing the train speeds is the dynamic amplification of stresses and displacements in the underlying ground and track layers at high train speeds. Several studies (Kaynia et al., 2000, Madshus and Kaynia, 2000) reported that, this dynamic response is due to resonance between the speed of the train and the traveling Rayleigh wave (R-wave) in the underlying ground. The train speed corresponding to this resonating condition is considered as the critical speed of the track. The critical speed is controlled by the properties of track superstructure and wave propagation in the embankment and track layers (Sheng et al., 2004, Costa et al., 2015).

At critical speed, the dynamic stress and displacement amplify and can often lead to passenger discomfort, rapid degradation of the track layers and train derailment, in the worst case. This amplification has been observed at a high-speed railway site in Ledsgard case (Madshus and Kaynia, 2001), where the Swedish high-speed train has experienced excessive vibrations approaching the critical speed of the alluvial subgrade. Other field studies (Nimbalkar et al., 2012, Indraratna et al., 2010a) reported an increase in the magnitude of vertical stress in the track layers when the train speed increased. They also found that the amplification in dynamic response is also dependent on the stiffness of the underlying subgrade and train axle load.

Predicting the critical speed of railway tracks is very challenging and has been modeled by many researchers in the last two decades using various analytical, two dimensional (2D) and three dimensional (3D) numerical approaches. Numerical techniques include 2D Finite element models (Yang et al., 2009, Powrie et al., 2007), 2.5D FEM (Costa et al., 2015), 3D FEM (Connolly, 2013, Sayeed and Shahin, 2016) and Boundary element method (BEM) models (Correia dos Santos et al., 2017). Often 2.5D and 3D numerical models require high computational power, and the models are time-consuming. On the other hand, analytical approaches are comparatively faster with reasonable assumptions of the behavior of track elements. Some of the analytical approaches were developed using Euler-Bernoulli Beam on elastic foundation (Auersch, 1996), Timoshenko beam theory (Suiker et al., 1998, Chen et al., 2001, Sheng et al., 2004), and coupled vehicle-track interaction systems (Zhai et al., 1996,

Banimahd et al., 2012). However, these analytical models consider ballast and capping layers as discrete spring-dashpot elements and cannot adequately represent the dynamic stress conditions developed in these layers during the train passage. Some coupled analytical approaches were developed considering rheological models for rail, sleeper, and rail pads and considering the ballast layer as a continuous layer allowing for wave propagation (Suiker et al., 1999a, Suiker et al., 1999b). They presented that the layered track substructure behaves as a dispersive media for R-waves and the critical speed of the track is also found to be dependent on the particle size of ballast aggregates and thickness of the ballast layer along with the elastic properties of the material.

In addition to vertical stresses, the longitudinal and shear stresses are also found to increase with train speeds, which lead to the rotation of principal stress axes in the underlying substructure layers (Yang et al., 2009, Powrie et al., 2007, Varandas et al., 2016). This dynamic stress amplification and principal stress rotation can cause rapid degradation of the granular layer (ballast and capping) and subgrade layers. Large scale triaxial testing of ballast (Indraratna et al., 2015, Indraratna et al., 2010b), Hollow Cylinder Apparatus (HCA) tests on subgrade soils (Gräbe and Clayton, 2009, Cai et al., 2018) and multi-laminate constitutive modelling of ballast (Malisetty et al., 2020b, Malisetty et al., 2020a) have reported that the permanent deformations of these materials under repeated loading conditions are exacerbated at higher dynamic loads. It is essential to include the permanent deformation response of track layers under dynamic loads imparted by trains to estimate the safe operating speed.

This paper presents a simple analytical approach based on Suiker et al. (1999a) to predict the stress and displacement response in the track, considering the ballast layer as a continuous medium. The influence of different parameters such as stiffness, thickness and fouling of the ballast layer are discussed. Further, the dynamic stress response is compared with the peak static deviatoric strength of ballast to estimate the allowable train speed for the optimal performance of track layers.
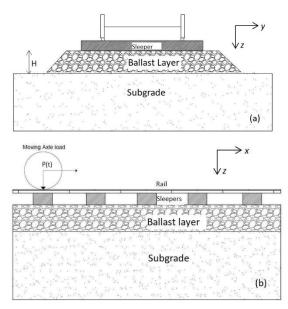

Figure 1 (a) Cross-sectional view and (b) longitudinal view of railway track

2 ANALYTICAL MODEL

A typical ballasted railway track is composed of two parallel beams placed on sleepers resting on the track substructure. A two-layered substructure is considered with a ballast layer at the top overlying a semi-infinite subgrade layer. The equivalent stiffness of the layers beneath the ballast layer is computed and taken as the stiffness of subgrade. For analysing the model, the longitudinal, lateral, and vertical directions of the track are considered as x, y and z, respectively. The rail movement and stresses are considered positive (+) and negative (-) in the downwards and upward directions.

2.1 Superstructure

The track superstructure system composes of rail, rail pads and sleepers. In this paper, rail is considered as Euler-Bernoulli beam and rail pads are considered as a spring-dashpot system (Figure 2). The train axle loading $P(t)$ is considered as a harmonic load (see Eq. 1), with a frequency $\omega_l = 2\pi V/L$ equivalent to the train speed $V(m/s)$, where L=1.72m is the minimum axle-axle distance as defined in Indraratna and Salim (2005).

$$P(t) = P_0 g \cos(\omega_l t) \qquad (1)$$

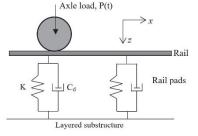where, P_0 is the static wheel load and g is the acceleration due to gravity (9.8 m/s2)

Figure 2. Rheological model of the superstructure of the railway track

The differential equation for the rail displacement $z_r(x,t)$ of the rail can be given as (Esveld, 2001):

$$E_r I_r \frac{\partial^4 z_r}{\partial x^4} + M \frac{\partial^2 z_r}{\partial t^2} + C_d \frac{\partial z_r}{\partial t} + K z_r = P(t) \qquad (2)$$

Where, E_r and I_r are Young's modulus, and the second moment of inertia of the rail, M is the mass of the sleeper and rail together, K and C_d are the stiffness and damping coefficient of the rail pad, respectively. The dynamic load transmitted by the superstructure system to the ballast layer at the sleeper-ballast interface can be computed using:

$$P_T(t) = P_0 g T_d \cos(\omega_l t) \qquad (3)$$

Where, T_d is the superstructure load transmissibility factor given as:

$$T_d = \sqrt{K^2 + (C_d \omega_l)^2} / \sqrt{(K - M_r \omega_l^2)^2 + (C_d \omega_l)^2} \qquad (4)$$

2.2 Substructure

The dynamic load transmitted by the superstructure generates R-waves in the ballast and subgrade layers. To determine the amplitude of R-waves generated in the track substructure, the P-wave and SV wave potentials in the ballast and subgrade layers are combined using appropriate boundary conditions (Suiker et al., 1999a). By considering the conservation of translation momentum during R-wave propagation, the Cauchy stresses at a depth z in the ballast layer under an excitation load are given as:

$$\sigma_{zz}^1 = e^{-i(\omega t - kx)}\left\{b_1 A_{p1}^1 e^{i\xi_{p1}^1 Z} + b_2 A_{s1}^1 e^{i\xi_{s1}^1 Z} + b_1 A_{p2}^1 e^{i\xi_{p2}^1 Z} - b_2 A_{s2}^{(1)} e^{i\xi_{s2}^{(1)} Z}\right\} \tag{5}$$

$$\sigma_{xx}^1 = e^{-i(\omega t - kx)}\left\{b_3 A_{p1}^1 e^{i\xi_{p1}^1 Z} - b_2 A_{s1}^1 e^{i\xi_{s1}^1 Z} + b_3 A_{p2}^1 e^{i\xi_{p2}^1 Z} + b_2 A_{s2}^1 e^{i\xi_{s2}^1 Z}\right\} \tag{6}$$

$$\sigma_{zx}^1 = e^{-i(\omega t - kx)}\left\{b_4 A_{p1}^1 e^{i\xi_{p1}^1 Z} + b_5 A_{s1}^1 e^{i\xi_{s1}^{(1)} Z} - b_4 A_{p2}^1 e^{i\xi_{p2}^1 Z} + b_5 A_{s2}^1 e^{-i\xi_{s2}^1 Z}\right\} \tag{7}$$

where, σ_{zz}^1, σ_{xz}^1 and σ_{xx}^1 are the vertical, shear and longitudinal stresses, respectively. The expressions for ballast and subgrade layers are represented with superscript 1 and 2, respectively. The instantaneous longitudinal (u_x^1) and vertical (u_z^1) displacements in the ballast layer can be written as:

$$u_x^1 = -i e^{-i(\omega t - kx)}\left\{k A_{p1}^1 e^{i\xi_{p1}^1 Z} + k A_{p2}^1 e^{i\xi_{p2}^1 Z} + \xi_{s1}^1 A_{s1}^1 e^{i\xi_{s1}^1 Z} - \xi_{s2}^1 A_{s2}^1 e^{i\xi_{s2}^1 Z}\right\} \tag{8}$$

$$u_z^1 = i e^{-i(\omega t - kx)}\left\{\xi_{p1}^1 A_{p1}^1 e^{i\xi_{p1}^1 Z} - \xi_{p2}^1 A_{p2}^1 e^{i\xi_{p2}^1 Z} - k A_{s1}^1 e^{i\xi_{s1}^1 Z} - k A_{s2}^1 e^{i\xi_{s2}^1 Z}\right\} \tag{9}$$

Similarly, the dynamic stresses and displacements in the subgrade layer can be written as:

$$\sigma_{zz}^2 = e^{-i(\omega t - kx)}\left\{b_6 A_{p1}^2 e^{i\xi_{p1}^2 Z} + b_7 A_{s1}^2 e^{i\xi_{s1}^2 Z}\right\} \tag{10}$$

$$\sigma_{xx}^2 = e^{-i(\omega t - kx)}\left\{b_8 A_{p1}^2 e^{i\xi_{p1}^2 Z} - b_7 A_{s1}^2 e^{i\xi_{s1}^2 Z}\right\} \tag{11}$$

$$\sigma_{zx}^2 = e^{-i(\omega t - kx)}\left\{b_9 A_{p1}^2 e^{i\xi_{p1}^2 Z} + b_{10} A_{s1}^2 e^{i\xi_{s1}^2 Z}\right\} \tag{12}$$

$$u_x^2 = -i e^{-i(\omega t - kx)}\left\{k A_{p1}^2 e^{i\xi_{p1}^2 Z} + \xi_{s1}^2 A_{s1}^2 e^{i\xi_{s1}^2 Z}\right\} \tag{13}$$

$$u_z^2 = i e^{-i(\omega t - kx)}\left\{\xi_{p1}^2 A_{p1}^2 e^{i\xi_{p1}^2 Z} - k A_{s1}^2 e^{i\xi_{s1}^2 Z}\right\} \tag{14}$$

In Eqs. 5-9, A_{p1}^1, A_{p2}^1 and A_{s1}^1, A_{s2}^1 represent the amplitudes of P-wave and S-wave potentials in the ballast layer, respectively. In Eqs. 10-14, A_{p1}^2 and A_{s1}^2 represent the amplitudes of P-wave and S-wave potentials in the subgrade layer, respectively. ω and k are the angular frequency and wavenumber of the R-waves generated in the substructure. The parameters b_1 to b_{10} are functions of Elastic modulus and poisons ratio of ballast and subgrade layers, and the derivations are given in Suiker et al. (1999a). The parameters $\xi_{p1}^1, \xi_{p2}^1, \xi_{p1}^2$ and $\xi_{s1}^1, \xi_{s2}^1, \xi_{s1}^2$ are the depth attenuation factors for P and SV waves given as:

$$\xi_{p,s,1,2}^{(1)} = = \pm\sqrt{\frac{\omega^2}{C_{p,s}^2} - k^2} \tag{15}$$

where, C_p and C_s are the P-wave and S-wave velocities, respectively. The dynamic stresses and displacements in Eqs. 6-14 contain 6 unknown amplitude parameters, which can be determined using the boundary conditions for R-wave propagation. For the assumed track substructure, the following boundary conditions are considered: At the free surface of the ballast layer ($z = -H$) (See Figure 1a), the vertical stress is equal to the stress imparted by the sleeper with no shear stress and can be given as:

$$\sigma_{zz}^1 = \frac{P_T(t)}{A_{sleeper}} \tag{16a}$$

$$\sigma_{zx}^1 = 0 \tag{16b}$$

where, $A_{sleeper}$ is the sleeper-ballast interface contact area. And at the ballast-subgrade layer interface i.e., at $z = 0$, the stress and displacement compatibility is considered and can be given as:

$$\sigma_{zz}^1 = \sigma_{zz}^2 \tag{17a}$$

$$\sigma_{zx}^1 = \sigma_{zx}^2 \tag{17b}$$

$$u_x^1 = u_x^2 \tag{17c}$$

$$u_z^1 = u_z^2 \tag{17d}$$

Substituting the expressions for stresses and displacements (Eqs.5-14) in the boundary conditions (Eqs.16-17) yield the amplitudes of wave potentials as a function of ω, k and thickness of the ballast layer (H). It is to be noted that a unique critical frequency or critical speed does not exist in layered media as observed in a homogenous half-space. The mode of propagation of R-wave governs the dynamic response in layered media due to the dispersive nature of the R-waves (Suiker et al., 1999b).

3 INFLUENCE OF TRAIN SPEED ON TRACK DYNAMIC RESPONSE

Using the analytical method, the stress and displacement response of a model track is predicted. The material properties of different components of the railway track considered for the analysis are shown in Table-1. Standard 60 kg steel rail and studded rubber pads with stiffness and damping properties from Kaewunruen and Remminikov (2009) are considered in this study. The substructure properties are taken for the railway track on sections with alluvial subgrade at Singleton, NSW (Nimbalkar and Indraratna 2016). The elastic modulus of ballast layer is back calculated from the shear wave velocities obtained from MASW testing on NSW tracks by Anbazhagan et al. (2011). At Singleton, ballast layer was underlain by subballast (150 mm), formation (400 mm) and alluvial clay layers. For this analysis, the multi-layered subgrade system is simplified using a composite subgrade layer with an equivalent elastic modulus (Indraratna and Ngo 2018).

Table 1. Material properties

Property	Symbol (units)	Current study
Rail beam		
Mass per unit beam length	M (kg/m)	60
Elastic modulus of rail	E_r (N/m^2)	207*10^9
Moment of inertia	I_r (m^4)	3.04*10^{-5}
Rail pads		
Stiffness	K (N/m)	65*10^6
Damping coefficient	C_d (N.s/m^2)	10*10^4
Ballast		
Elastic modulus	E_b (N/m^2)	85
Poissons ratio, density	v_s, ρ_s (kg/m^3)	0.35, 1530
Subgrade		
Elastic modulus	E_s (N/m^2)	30*10^6
Poissons ratio, density	v_s, ρ_s (kg/m^3)	0.4, 2000

Figure 3 shows the validation of the analytical model with the measured sleeper-ballast interface vertical stresss at different train speeds at Singleton NSW. The model predictions showed a good comparison of dynamic stresses with the field data for 25T axle load in the speed range of 30-80 kmph and the amplification trends match quite closely. However, the amplification for 30T axle load observed in the field data is slightly higher then the model predictions. This can be due to the influence of impact loads coming from wheel irregularities at higher axle loads which can lead to rapid degradation of ballast, constantly changing its elastic properties and this behavior is not considered in the current model.

Figure 4 shows the model predictions of the variation of dynamic vertical displacement of the rail with increasing train speeds. The dynamic vertical displacement of the rail is governed by the response of the spring-damper superstructure system (Eq. 3) in interaction with the wave propagation in the layered substructure (Eq. 10). It can be observed that the displacements

increased with train speed till reaching maximum and the corresponding train speed can be considered as the critical speed of the track (V_c). When train speeds are below $0.5\,V_c$, the amplification of vertical displacements is minimal and can be considered as quasi-static speed zone ($V < 0.5V_c$). However, as the train speeds crossed $0.5\,V_c$ and entered subcritical zone ($0.5V_c < V < V_c$), the dynamic stresses increased rapidly till reaching maximum at V_c. This amplification in response is due to the resonance between the train speed and track. For a 300 mm thick ballast layer, V_c is found to be 290 kmph approximately. It is important to observe that as the thickness of the ballast layer increased from 300mm to 600 mm, V_c increased from 290 kmph to 360 kmph and the rate of amplification of displacements reduced. In addition, the peak rail displacement at critical speed reduced with increase in thickness of ballast layer.
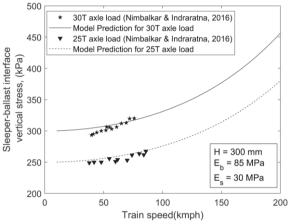

Figure 3. Dynamic sleeper-ballast interface vertical stress at different train speeds: model predictions compared with field measurement from Nimbalkar and Indraratna (2016)
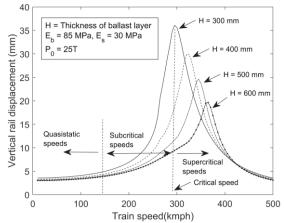

Figure 4. Dynamic vertical displacement response of rail at different train speeds

To understand the influence of train speeds on stresses in the ballast layer, the dynamic vertical stress response at the mid-depth of the ballast layer (for H = 300mm and P_0 = 25T) is considered as shown in Figure 5. The predictions clearly show that the vertical stress amplification in the ballast layer with train speeds follows a similar pattern to the dynamic rail displacements. For a constant stiffness of the ballast layer, when the stiffness of the underlying subgrade is increased from 20 MPa to 40 MPa, V_c increases from 290 kmph to 320 kmph. Despite the constant axle load, the peak vertical stress in the ballast layer for a stiffer subgrade (E_b = 40 MPa) is higher than that for a softer subgrade (E_b = 20 MPa). This implies that more dynamic energy is induced in the ballast layer in the case of stiffer subgrade than with a softer subgrade layer. It is also to be noted

that, during a certain speed interval, the vertical stresses for the track with a softer subgrade are higher than those of the track with a stiffer subgrade. This behavior can be due to the reason that the train speed for the case of softer subgrade has reached a critical zone ($\sim V_c$), while the same train speed for stiffer subgrades is still in the subcritical zone.
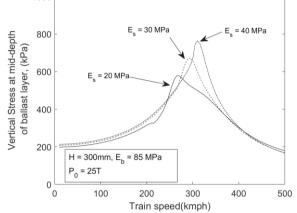

Figure 5. Dynamic vertical stress response in the mid-depth of the ballast layer at different train speeds
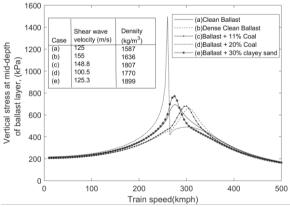

Figure 6. Effect of vertical stress at mid-depth of ballast layer for different ballast layer fouling. Shear wave velocity and density data sourced from Anbazhagan et al. (2011)

In Australia, often ballasted railway tracks are fouled with coal, sandy clay or broken ballast aggregates reducing the shear strength of the ballast layer (Anbazhagan et al., 2011). To evaluate the influence of fouling on the critical speed of the track, the elastic modulus of ballast is varied for different clay and clayey sand fouling percentages, as shown in Figure 6. All the other parameters (E_s=30 kPa, H=300 mm, P_0=25T) are kept constant for all the cases. The densities and shear wave velocities for fouled ballast are obtained from Anbazhagan et al. (2011). As seen from Figure 6, two types of clean ballast: (a) medium dense and (b) dense, two types of coal fouling: (c) 11% and (d) 20%, and (e) 30% clayey sand fouling are considered. The track with dense clean ballast is found to have the highest critical speed (V_c = 300 kmph), while the track with 20% coal fouled ballast has the lowest critical speed (V_c = 250 kmph). Also, the vertical stress amplification is higher for the case of 20% coal fouled ballast and is almost twice that of other cases when train speed approached V_c.

For the case of clean ballast (a) and ballast with 30% clayey sand (e), the critical speeds (V_c = 275 kmph) are computed to be almost similar, which is mainly due to a similar shear wave velocities for both cases. However, the vertical stresses at critical speed are higher for the case with clay fouled sand, which can be due to its higher density. Also, it is interesting to note that the track with 11% coal fouled ballast performed better than clean

ballast. As described in Anbazhagan et al. (2011), the addition of a small quantity of fines will initially increase the stiffness of the ballast, causing the shear wave velocity to increase, hence increasing the critical speed.

4 PERMANENT DEFORMATION OF TRACK MATERIALS UNDER DYNAMIC LOADS

The dynamic vertical stresses generated in ballast layer are dissipated through degradation and permanent deformations in ballast layer. So, the estimation of critical speed should also include the performance of ballast under these dynamic stresses. For optimum performance, the dynamic stresses at high train speeds should not exceed the peak static deviatoric strength of ballast, otherwise, can lead to excessive deformations and particle breakage and require frequent maintenance than expected. The model predictions of stress vs train speed are compared with the peak static deviatoric strength of railway ballast, which governs the permanent deformations under repeated loads and is shown in Figure 7. The stress response for two types of axle loads: 25T and 30T, and peak static shear strength at different confining stresses are considered. As seen in Figure 7, there is no significant change in the critical speed of the track with increase in axle load when only dynamic stresses are considered, however the magnitude of vertical stress is higher for higher axle loads. To capture the influence of in-situ confining stress, the peak static strength at two different confining stresses (30 and 60 kPa) are superimposed on the dynamic stress curves. The intersection points denote the train speed at which the dynamic stresses become higher than the peak strength of ballast layer and can be termed as limiting speed (V_l).

From Figure 7, it can be seen that V_l is significantly lower than that of V_c and varies with axle load in contrast to V_c. For the track with 300 mm thick ballast layer and at confining stress (σ_3') of 30 kPa, V_l limits to 180 kmph for 25T axle load, when compared to V_c of 290 kmph. It can also be observed that, by increasing σ_3' from 30 kPa to 60 kPa, V_l can be increased to 270 kmph and 245 kmph for 25T and 30T axle load trains, respectively. This implies that the limiting speed for higher axle loads is lower than that for lowe axle loads. Further, increasing the thickness of the ballast layer to 500 mm is also found to reduce the dynamic stress and increase V_c. For σ_3' =30 kPa, V_l is found to be 270 kmph and 220 kmph for 25T and 30T axle load trains, respectively. By using the combination of increased ballast layer thickness and high confining stresses, V_l can be increased to 330 kmph and 300 kmph for 25T and 30T axle load trains, respectively.

4 CONCLUSIONS

In this paper, a simple analytical model is presented considering the influence of Rayleigh wave propagation on the dynamic stresses in the ballast layer. The dynamic amplification of displacements and stresses in the track are analysed under different loading and subgrade conditions. The model is validated with field data from Singleton, NSW and the predictions showed a good agreement with measured data. The amplification of dynamic displacements and stresses was found to be low till the train speeds approached $0.5V_c$, however, a rapid increase in amplification was observed when train speed V_c. Increasing the thickness of the ballast layer not only increased the critical speed of the track but also reduced the magnitude of dynamic stresses in the ballast layer. While increasing the stiffness of the subgrade layer increased the critical speed, the magnitude of dynamic stresses in the ballast layer also increased. Also, ballast fouling was found to influence the critical train speed, especially for the cases of 20% coal fouling and 30% clayey sand fouling. The reduction in the critical speed is particularly important on railway tracks where mud pumping and coal fouling phenomena occur regularly and can affect the dynamic response of the track.

In addition to the critical speed of the track, the importance of limiting train speed based on the peak strength of the ballast layer was discussed. The critical speed was found to be constant for different axle loads; however, the magnitude of stresses and displacements was higher for higher axle loads. In contrast, the limiting train speed is lower for heavy haul freight trains when compared to passenger trains and was much lower than that of critical speed. In practice, the consideration of the ballast layer as a continuous medium allows the estimation of dynamic stresses induced in the ballast layer. It is also important in designing the thickness and layer stiffness in high-speed railway tracks to minimise the maintenance costs of the ballast layer. Further, track improvements such as increasing the confining stress and thickness of the ballast layer can increase the limiting train speeds by 30% to 40% depending on the track superstructure and substructure properties.

5 ACKNOWLEDGEMENTS

6 REFERENCES

ANBAZHAGAN, P., INDRARATNA, B. & AMARAJEEVI, G. 2011. Characterization of Clean and Fouled Rail Track Ballast Subsurface Using Seismic Surface Survey Method: Model and Field Studies. *Journal of Testing and Evaluation,* 39**,** 831-841.

AUERSCH, L. 1996. Dynamic plate-soil interaction—finite and infinite, flexible and rigid plates on homogeneous, layered or Winkler soil. *soil dynamics and earthquake engineering,* 15**,** 51-59.

BANIMAHD, M., WOODWARD, P. K., KENNEDY, J. & MEDERO, G. M. Behaviour of train–track interaction in stiffness transitions. Proceedings of the Institution of Civil Engineers-Transport, 2012. Thomas Telford Ltd, 205-214.

CAI, Y., WU, T., GUO, L. & WANG, J. 2018. Stiffness degradation and plastic strain accumulation of clay under cyclic load with principal stress rotation and deviatoric stress variation. *Journal of Geotechnical and Geoenvironmental Engineering,* 144**,** 04018021.

CHEN, Y. H., HUANG, Y. H. & SHIH, C. T. 2001. Response of an infinite Timoshenko beam on a viscoelastic foundation to a harmonic moving load. *Journal of Sound and Vibration,* 241**,** 809-824.

CONNOLLY, D. 2013. *Ground borne vibrations from high speed trains.*

CORREIA DOS SANTOS, N., BARBOSA, J., CALÇADA, R. & DELGADO, R. 2017. Track-ground vibrations induced by railway
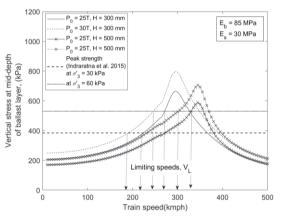
Figure 7. Comparison of dynamic stresses with peak static deviatoric strength of ballast at different train speeds, Peak strength data sourced from Indraratna et al. (2015)

traffic: experimental validation of a 3D numerical model. *Soil Dynamics and Earthquake Engineering, 97,* 324-344.

COSTA, P. A., COLAÇO, A., CALÇADA, R. & CARDOSO, A. S. 2015. Critical speed of railway tracks. Detailed and simplified approaches. *Transportation Geotechnics, 2,* 30-46.

ESVELD, C. 2001. *Modern Railway Track, 2nd Editon,* Delft university of Technology.

GRÄBE, P. & CLAYTON, C. 2009. Effects of principal stress rotation on permanent deformation in rail track foundations. *Journal of Geotechnical and Geoenvironmental Engineering, 135,* 555-565.

INDRARATNA, B., & NGO, T. 2018. *Ballast Railroad Design: SMART-UOW Approach* (1st ed.). CRC Press.

INDRARATNA, B., NIMBALKAR, S., CHRISTIE, D., RUJIKIATKAMJORN, C., VINOD, J. J. J. O. G. & ENGINEERING, G. 2010a. Field assessment of the performance of a ballasted rail track with and without geosynthetics. *Journal of Geotechnical and Geoenvironmental Engineering, 136,* 907-917.

INDRARATNA, B. & SALIM, W. 2005. *Mechanics of ballasted rail tracks: a geotechnical perspective*, CRC Press.

INDRARATNA, B., SUN, Q. D. & NIMBALKAR, S. 2015. Observed and predicted behaviour of rail ballast under monotonic loading capturing particle breakage. *Canadian Geotechnical Journal, 52,* 73-86.

INDRARATNA, B., THAKUR, P. K. & VINOD, J. S. 2010b. Experimental and numerical study of railway ballast behavior under cyclic loading. *International Journal of Geomechanics, 10,* 136-144.

KAYNIA, A. M., MADSHUS, C. & ZACKRISSON, P. 2000. Ground vibration from high-speed trains: prediction and countermeasure. *Journal of Geotechnical and Geoenvironmental Engineering, 126,* 531-537.

KAEWUNRUEN, S & REMENNIKOV, AM. 2009. State dependent properties of rail pads, Transport Engineering in Australia, 12(1), 17-24.

MADSHUS, C. & KAYNIA, A. 2000. High-speed railway lines on soft ground: dynamic behaviour at critical train speed. 231, 689-701.

MADSHUS, C. & KAYNIA, A. 2001. High-speed trains on soft ground: track–embankment–soil response and vibration generation. *Noise and vibration from high-speed trains.* Thomas Telford Publishing.

MALISETTY, R. S., INDRARATNA, B. & VINOD, J. 2020a. Behaviour of ballast under principal stress rotation: Multi-laminate approach for moving loads. *Computers and Geotechnics, 125,* 103655.

MALISETTY, R. S., INDRARATNA, B. & VINOD, J. S. 2020b. Multilaminate Mathematical Framework for Analyzing the Deformation of Coarse Granular Materials. *International Journal of Geomechanics, 20,* 06020004.

NIMBALKAR, S. & INDRARATNA, B. 2016. Improved Performance of Ballasted Railway Track Using Geosynthetics and Rubber Shockmat. 142, 04016031.

NIMBALKAR, S., INDRARATNA, B., DASH, S. K. & CHRISTIE, D. 2012. Improved performance of railway ballast under impact loads using shock mats. *Journal of Geotechnical and Geoenvironmental Engineering, 138,* 281-294.

POWRIE, W., YANG, L. & CLAYTON, C. R. Stress changes in the ground below ballasted railway track during train passage. Proceedings of the Institution of Mechanical Engineers, Part F: Journal of Rail and Rapid Transit, 2007. 247-262.

SAYEED, M. A. & SHAHIN, M. A. 2016. Three-dimensional numerical modelling of ballasted railway track foundations for high-speed trains with special reference to critical speed. *Transportation Geotechnics, 6,* 55-65.

SHENG, X., JONES, C. & THOMPSON, D. 2004. A theoretical study on the influence of the track on train-induced ground vibration. *Journal of Sound and Vibration, 272,* 909-936.

SUIKER, A., DE BORST, R. & ESVELD, C. 1998. Critical behaviour of a Timoshenko beam-half plane system under a moving load. *Archive of Applied Mechanics, 68,* 158-168.

SUIKER, A. S., CHANG, C. S., DE BORST, R. & ESVELD, C. 1999a. Surface waves in a stratified half space with enhanced continuum properties. Part 1: Formulation of the boundary value problem. *European Journal of Mechanics-A/Solids, 18,* 749-768.

SUIKER, A. S., CHANG, C. S., DE BORST, R. & ESVELD, C. 1999b. Surface waves in a stratified half space with enhanced continuum properties. Part 2: Analysis of the wave characteristics in regard to high-speed railway tracks. *European Journal of Mechanics-A/Solids, 18,* 769-784.

VARANDAS, J. N., PAIXÃO, A., FORTUNATO, E. & HÖLSCHER, P.

2016. A numerical study on the stress changes in the ballast due to train passages. *Procedia engineering, 143,* 1169-1176.

YANG, L., POWRIE, W. & PRIEST, J. 2009. Dynamic stress analysis of a ballasted railway track bed during train passage. *Journal of Geotechnical and Geoenvironmental Engineering, 135,* 680-689.

ZHAI, W., CAI, C. & GUO, S. 1996. Coupling model of vertical and lateral vehicle/track interactions. *Vehicle system dynamics 26,* 61-79.